[CANCER RESEARCH 63, 5266–5273, September 1, 2003]

Genome-wide Array CGH Analysis of Murine Neuroblastoma Reveals Distinct Genomic Aberrations which Parallel those in Human Tumors[1,2]

Christopher S. Hackett,[3] J. Graeme Hodgson,[2] Mark E. Law, Jane Fridlyand, Kazutoyo Osoegawa, Pieter J. de Jong, Norma J. Nowak, Daniel Pinkel, Donna G. Albertson, Ajay Jain, Robert Jenkins, Joe W. Gray, and William A. Weiss[4]

Departments of Neurology [C. S. H., W. A. W.], Pediatrics [C. S. H., W. A. W.], Neurological Surgery [C. S. H., W. A. W.], Laboratory Medicine [J. G. H., D. P., A. J., J. W. G., W. A. W.], Cancer Center [J. G. H., J. F., D. P., D. G. A., A. J., W. A. W.], and Cancer Research Institute [J. F., D. G. A., A. J., J. W. G.], University of California, San Francisco, California 94143-0114; Department of Laboratory Medicine and Pathology, Mayo Clinic and Foundation, Rochester, Minnesota 55905 [M. E. L., R. J.]; Children's Hospital Oakland Research Institute, BACPAC Resources, Oakland, California 94609-1809 [K. O., P. J. d. J.]; and Roswell Park Cancer Institute, Buffalo, New York 14263 [N. J. N.]

ABSTRACT

Neuroblastoma, the third most common tumor of childhood, is a complex disease in which few genetic mutations have been identified. Mice expressing a human *MYCN* oncogene driven by the rat tyrosine hydroxylase promoter (*TH-MYCN*) represent an animal model for this disorder. We performed microarray-based comparative genomic hybridization analysis on murine tumors, identifying gains on chromosomes 1, 3, 11, 14, 17, and 18 and losses on chromosomes 5, 9, and 16. Fluorescence *in situ* hybridization analysis confirmed an amplicon on chromosome 18 as the site of *TH-MYCN* transgene integration. Selected tumors with localized gains of chromosome 11 delineate a 15-Mb region orthologous to human chromosome 17q and help to narrow the minimal region gained in human tumors. We observed clustered loss of chromosomes 5, 9, and 16, orthologous to a similar pattern of combined loss of chromosomes 3p, 4p, and 11q in human tumors. These data demonstrate conservation of many genetic changes in murine and human neuroblastoma and suggest that further delineation of genetic abnormalities in murine tumors may identify genes important in human disease.

INTRODUCTION

Neuroblastoma, a tumor of sympathetic peripheral nervous tissue, is the third most common tumor of childhood, accounting for 15% of cancer-related deaths (1). Amplification of the *MYCN* gene is the only consistent genetic mutation described to date in neuroblastoma, occurring in ~30% of children with this disease and correlating with advanced stage and poor outcome (2). Numerous regions of loss of heterozygosity have been identified in tumors (reviewed in Ref. 1). CGH[5] has validated loss of chromosome regions 1p36, 3p, 4p, 9p, 11q, and 14q and frequent gains of chromosomes 17 or 17q and 18q (3). CGH has narrowed the regions of interest on these chromosomes to <25 Mb in some cases and implicated additional gains of chromosomes 1, 2, 6, 7, 12, and 13 (4–11). The best characterized regions of copy number abnormalities include loss of 1p36 in 19% of cases (12) and gain of 17q, which is also the most frequent genetic event, occurring in ≤83% of all tumors (3) and >90% of high-grade tumors (13). Loss of 1p36, gain of 17q, and amplification of *MYCN* show significant interaction and correlate with advanced tumors and poor outcome (3, 14).

Overexpression of the human *MYCN* oncogene driven by the rat tyrosine hydroxylase promoter causes tumors in transgenic mice, recapitulating several histological and pathological aspects of clinical neuroblastoma (15). Tumors from these mice localize to paraspinous ganglia and adrenal glands, stain for neuronal markers, show ultrastructural features of neurons (neurosecretory granules and synapses), and share with the human tumors a propensity to grow along radicular nerves. Previous genome-wide screens in these mice revealed a range of genetic aberrations. Chromosome CGH showed losses of mouse chromosomes 5, 9, 16, and X and gains of chromosomes 3, 11, and 17 (15). A low-resolution AI screen showed frequent imbalance on chromosomes 1, 3, 10, 11, 14, and 18 (16).

Array CGH based on hybridization of tumor DNA to genomic BACs provides a way to analyze genomic changes in tumor tissue with high sensitivity, detecting single-copy number aberrations in tissues in the presence of ≤60% contamination by normal tissue (17–20). Here, we used this technology to refine the genetic characterization of 40 murine neuroblastoma tumors, using an array comprised of 1056 BAC clones providing 5-Mb average resolution across the genome, and sub-Mb resolution in regions identified in previous genetic screens of transgenic tumor models (20). We have validated specific observations from our array CGH screen using FISH and through AI analyses. These studies revealed a wide range of genetic copy number changes in murine tumors, including localized gains of a segment of mouse chromosome 11 orthologous to human chromosome 17q, which narrows the region of clinical interest in human neuroblastoma to 18.5 Mb. In addition, this study identified genetic changes in other regions implicated in human disease and other animal models, suggesting a conserved interaction among the mouse orthologues of human chromosomes 3p, 4p, and 11q, which interact in advanced cases of human neuroblastoma.

MATERIALS AND METHODS

Tumor Generation and DNA Isolation. Tumors were dissected from a cross of transgenic *C57BL/6J* to wild-type *Mus musculus castaneus Ei* mice. All mice were obtained from The Jackson Laboratory (Bar Harbor, ME). Genomic DNA was isolated from frozen primary neuroblastomas by overnight digestion [50 mM Tris (pH 8.0), 1 mM EDTA (pH 8.0), 0.5% SDS, and 500 μg/ml Proteinase K; Roche, Indianapolis, IN)] followed by phenol-chloroform extraction and ethanol precipitation. DNA concentrations were quantified using a fluorometer (Amersham, Piscataway, NJ).

Array Preparation. BACs described previously (20), and additional BACs isolated from the RPCI-23 mouse BAC library (21), were organized into 96-well plates. Each BAC contained a known sequence-tagged site marker, gene, or BAC end sequence, which was used to place it on the assembled mouse genome sequence using batch BLAT (22). All genomic coordinates described in this study are based on the February 2002 freeze of the assembled mouse genome available through the UCSC Genome Browser.[6] A detailed list of the BAC clones used for these arrays, their associated markers, and genomic coordinates are also available online (see supplementary data). Single colonies

Received 3/3/03; revised 5/28/03; accepted 6/16/03.

The costs of publication of this article were defrayed in part by the payment of page charges. This article must therefore be hereby marked *advertisement* in accordance with 18 U.S.C. Section 1734 solely to indicate this fact.

[1] W. A. W. was supported by National Institute of Neurological Disorders and Stroke Grant K02NS0226 and by grants from the March of Dimes and Concern Foundations. G. H. was supported by the Department of Defense Grant DAMD17-01-1-0187.

[2] Supplementary data for this article are available at Cancer Research Online (http://cancerres.aacrjournals.org).

[3] C. S. H. and J. G. H. contributed equally to this manuscript.

[4] To whom requests for reprints should be addressed, at Department of Neurology, Box 0114, Room C-215, San Francisco, CA 94143-0114. E-mail: weiss@cgl.ucsf.edu.

[5] The abbreviations used are: CGH, comparative genomic hybridization; AI, allelic imbalance; FISH, fluorescence *in situ* hybridization; BAC, bacterial artificial chromosome.

[6] Internet address: http://genome.ucsc.edu.

were isolated from each BAC clone on LB plates containing 20 μg/ml chloramphenicol. A single colony per clone was arrayed into 96-well format, and DNA was prepared with automated instrumentation (Autogen960; Holliston, MA) using the standard BAC preparation protocol, typically yielding ~200 ng of BAC DNA, which was resuspended to a final concentration of ~5–10 ng/μl. Two microliters of BAC DNA were used for amplification by DOP-PCR (23). Printing onto 3D-Link activated slides (Motorola Life Sciences, Pasadena, CA) was performed as described. Clones were printed in quadruplicate (two spatially separated duplicates). Two arrays were printed per slide, each 12 mm × 12 mm in size.

Array Hybridization. Array CGH was performed essentially as described (20). Briefly, 1 μg of *Dpn*II-digested tumor DNA and reference DNA (derived from the spleen, brain, or heart of the same animal as the tumor) was labeled with Cy3 or Cy5, respectively (Amersham, Piscataway, NJ) using the Bioprime random-primed labeling kit (Invitrogen, Carlsbad, CA). Unincorporated nucleotides were removed using Sephadex G-50 columns (Amersham, Piscataway, NJ), and tumor and reference samples were combined, precipitated with 50 μg of mouse Cot-1 DNA, and resuspended in 60 μl of hybridization solution (10% dextran sulfate, 50% formamide, 2 × SSC, 4% SDS, and 10 μg/μl yeast tRNA). Preannealed DNA samples were then applied to arrays fitted with 2.4 cm^2 EasiSeal gaskets (Continental Lab Products, San Diego, CA). Slides were placed in individual, prewarmed hybridization chambers (plastic slide holders) containing Whatmann paper soaked with 750 μl of 2 × SSC, 0.1% SDS to prevent evaporation and hybridized for a minimum of 36 h at 37°C on a slowly rocking platform. After hybridization, slides were washed, counterstained with 4′,6-diamidino-2-phenylindole, and imaged using a custom-built CCD camera (18). TIFF images were segmented, and spot statistics were calculated using custom software (24).

Analysis of array CGH profiles and determination of gain and loss thresholds were performed as described (20). Genomic profiles of $\log_2$ fluorescence ratios from each array CGH analysis were normalized to a median 0, where the median was computed over all clones on the array with the exception of the localized regions of high-density clone coverage on chromosomes 4, 6, 9, and 16. Clones mapping to these regions contained about half of the clones present on the array and were excluded because localized changes in these regions would violate the assumption for normalization to the median that either: (*a*) the majority of the clones do not change, or (*b*) the gain and loss occur at the same frequency (25). A mixture of three Gaussian distributions (corresponding to the normal, gained, and deleted portions of the tumor genome) was fit to a histogram of the ratios for each tumor using a hybrid least-squares/maximum likelihood method using the Solver tool in Microsoft Excel. Only 2 of the 40 tumors (5%) showed SDs of the central peak > 0.15. Clones with mean ratios falling 3 SD above or below the mean of the central (*i.e.* normal) distribution were scored as gained or lost, respectively.

Statistical Analysis. Clones scored present in <70% of tumors were filtered out for whole-chromosome analysis. This filtering removed ~13% of clones, leaving 845 with confirmed map positions on the February 2002 genome assembly. For whole-chromosome association analysis, a chromosome was scored as gained or lost if: (*a*) 90% of all clones on the chromosome had a $\log_2$ ratio greater or less than 0, respectively; and (*b*) the median of the $\log_2$ ratios of all clones on that chromosome was greater or less than 0.1 or −0.1, respectively. The main requirement that ≥90% of clones had to be greater or less than 0 may be justified by the following calculation: assuming that all of the clones on a given chromosome are at the same copy number and there are >10 clones/chromosome, we wanted to test a null hypothesis of diploid copy number or that the probability of $\log_2$ ratio being greater or less than 0 is 0.5. Using a normal approximation for comparing two binomial proportions (26), we calculated the probability of observing ≥90% of the clones being greater or less than 0 under the null hypothesis to be <0.005. Because we test 20 chromosomes in 40 samples, we expect to observe four false positives or fewer in the whole data set (<0.005 × 20 × 40). The requirement of minimum median aberration of $\log_2$ 0.1 is an ad-hoc one to make this procedure even more conservative and allows detection of changes present in only a small but non-negligible subset of genetically nonhomogenous cells (as the decrease of magnitude of $\log_2$ ratios with the proportion of cells with a given aberration has been investigated previously; Ref. 20), *e.g.*, assuming 20% admixture of the normal cells, the $\log_2$ ratio of 0.1 corresponds to ~20% of the tumor cells gaining a copy of the chromosome. We then manually examined the chromosomes assigned "change" status on which not all clones were above or <0 and eliminated three cases where a small contiguous part of chromosome was not aberrant, *i.e.*, the $\log_2$ ratios in that region randomly fluctuated ~0. These cases had passed 90% criterion because of the uneven coverage of the chromosomes on the array. We further analyzed only those chromosomes that were gained or lost in at least four samples. Thus, chromosomes 2, 4, 7, 10, 12, 13, and 19 were excluded from further analysis. All but three (15, 18, and X) of the remaining 13 chromosomes showed gains or losses exclusively. On 15, 18, and X, we recoded the less frequent events as "no change" (these events were singular except for X, which was gained in two cases and lost in seven). Remaining values were then coded as "1" for change and "0" for no change.

We then performed two-dimensional clustering of sample profiles (based on individual clones) and chromosomes (based on scores for whole-chromosome change). The chromosomes were clustered using agglomerative hierarchical average clustering with a binary metric in the "MVA" package in the R environment (27), which can be freely downloaded from the Internet.[7] The chromosomes were coded with 0s and 1s where "1" indicated that chromosome was gained or lost in a given sample and "0" otherwise. The dissimilarity between a pair of chromosomes was defined using a binary metric, *i.e.*, as proportion of samples in which only one of the chromosomes showed change among the samples in which at least one did. The samples were then ordered with agglomerative hierarchical average clustering using (1-pearson) correlation as a metric. Here, the $\log_2$ ratios for the clones mapped to the chromosomes in the clustering diagram were used to compute the distance matrix for the samples (28).

Interactions were assessed by performing one-sided Fisher exact tests for concordance on pairs of chromosomes using their binary codes for "change" *versus* "no change." Interaction between chromosomes 1 and 3 was not adjusted for multiple comparisons, as a previous study had suggested that they acted together. For all other pairs of chromosomes, scores were adjusted for multiple comparisons. The correction was done using a minP multiple testing procedure (as described in Ref. 29), which provides strong control of the family-wise Type I error rate. The permutation procedure was performed by randomly shuffling the chromosomal scores across samples and recomputing the Fisher exact *P* for each pair of chromosomes. For three-way interactions, a similar test was done, in which chromosome pairs were recoded as "1" if both changed and "0" otherwise, and each pair was then compared with the remaining chromosomes. If the chromosomal interactions we observed were simply caused by global chromosome instability, then the likelihood that a specific chromosome would show gain or loss should be identical for all chromosomes. Alternatively, if such chromosomal interactions were the result of specific selection, then the likelihood that a specific chromosome would show gain or loss should be different for specific chromosomes. To address whether the chromosomes that changed in more than four tumors had a homogeneous rate of change, we applied a test for homogeneity of binomial samples to such chromosomes (27). We obtained a $P < 0.0002$, thereby refuting the hypothesis of global instability in the absence of selection.

AI Analysis. Tumor DNA from 32 mice included in the array CGH screen was screened for AI using SSLP microsatellite markers across chromosomes 1, 3, 10, 11, 14, and 18, with additional control markers on chromosomes 2 and 13 (see supplementary data). PCR was run as described (16). Intensity of PCR bands was quantified using an ABI 377 fluorescence-based DNA sequencer (UCSF Genomics Core Facility) and analyzed using Genescan software (PE Biosystems, Foster City, CA). Ratios of band intensities for the two alleles of each marker were calculated and compared with the average ratio of 10 spleen samples for the same marker. Ratios of single markers in tumors with either <0.65 or >1.5 times the 10-spleen average were scored as imbalanced (30, 31).

FISH Analysis. BAC DNA (Research Genetics, Carlsbad, CA) from clones RP23-101G23, RP23-426C22 (chromosome 4), RP23-16A3 (chromosome 18), RP23-18M23, and RP23-301L12 (controls) was prepped using the Plasmid Mini kit (Roche, Indianapolis, IN). Probes were prepared from BAC DNA using the Vysis nick translation kit according to the manufacturer's protocol (Vysis, Inc., Downers Grove, IL). The *NMYC* transgene was detected using the Vysis human *NMYC* cDNA probe labeled with digoxigenin and detected with fluorescein antidigoxigenin (Roche, Indianapolis, IN). Probes

[7] Internet address: www.r-project.org.

were hybridized to primary fibroblast cultures and sections prepared from frozen normal and tumor tissues. Primary fibroblasts were isolated from freshly cut mouse tails and cultured and harvested using standard cytogenetic techniques. Frozen section slides were incubated in 75 mM KCl for 20 min, then Carnoy solution (3:1 methanol:acetic acid) for another 20 min, and dried at room temperature. The frozen section slides, and slides derived from the fibroblast cultures were then heated for 10 min at 90°C, incubated in Pepsin at 37°C for 30–60 s, washed in 70% ethanol for 30 s, and incubated in 2 × SSC at 37°C for 60 min. Slides were dried using an ethanol series (70%, 85%, 1 min each, and 100% for 10 min) followed by jet air drying. Slides were then incubated in 70% formamide at 70°C for 1 min and dried again through the same ethanol series (70%, 85%, 100%, and 1 min each) and jet dried. Probes were then denatured, added to slides, and incubated under a sealed coverslip for ≥12 h at 37°C. After hybridization, coverslips were removed, and slides were washed in 0.4 × SSC at 70°C for 2 min, rinsed in room temperature with 2 × SSC/0.1% NP40, jet air dried, and counterstained. Cells were viewed using an epifluorescence microscope equipped with Texas red/FITC/4′,6-diamidino-2-phenylindole filters.

RESULTS

Array CGH in Tumors from *TH-MYCN* Transgenic Mice. Mice transgenic for *MYCN* were back-crossed serially to nontransgenic mice of strain C57BL/6J. Starting at the F7 back-cross into C57BL/6J, transgenic females were crossed to *castaneus* males, because in our hands, *castaneus* females are poor mothers. Twenty-three tumors described previously (16) were included in this analysis, with back-cross ranging from F7 to F10. An additional 17 animals added to this study were derived from back-crossed mice ranging from F10 to F15. Mice were euthanized when tumors were visible or when mice were symptomatic (32). The histological characteristics of tumors in these animals were identical to those described previously.

Individual tumor hybridizations illustrated a range of genetic aberrations; combinations of whole chromosome gains and losses, localized gains and losses, and two tumors showing no identifiable genetic changes. Fig. 1*A* shows a tumor with whole-chromosome gains of chromosome 1 and 3. The higher ratios shown by clones on chromosome 3 relative to clones on chromosome 1 suggest that a single gain of chromosome 3 is more frequent in cells within the tumor population or that cells tended to have more copies of chromosome 3 relative to chromosome 1. Fig. 1*B* shows a tumor with gains of chromosomes 1, 3, 6, 11, and 17, localized gain on chromosome 8, loss of chromosomes 5, 9, and 16, and localized loss of distal chromosome 4. Fig. 1*C* shows localized gain on chromosome 8, amplification on distal chromosome 18, and an interstitial deletion on chromosome 16.

We used FISH to verify loss of distal chromosome 4 in the tumor analyzed in Fig. 1*B* using a BAC probe located within the region of loss observed by array CGH (Fig. 2*A*). Similarly, Fig. 2*B* confirms the amplification on chromosome 18 using a BAC corresponding to the peak of the amplicon in the tumor profiled in Fig. 1*C*. An ongoing

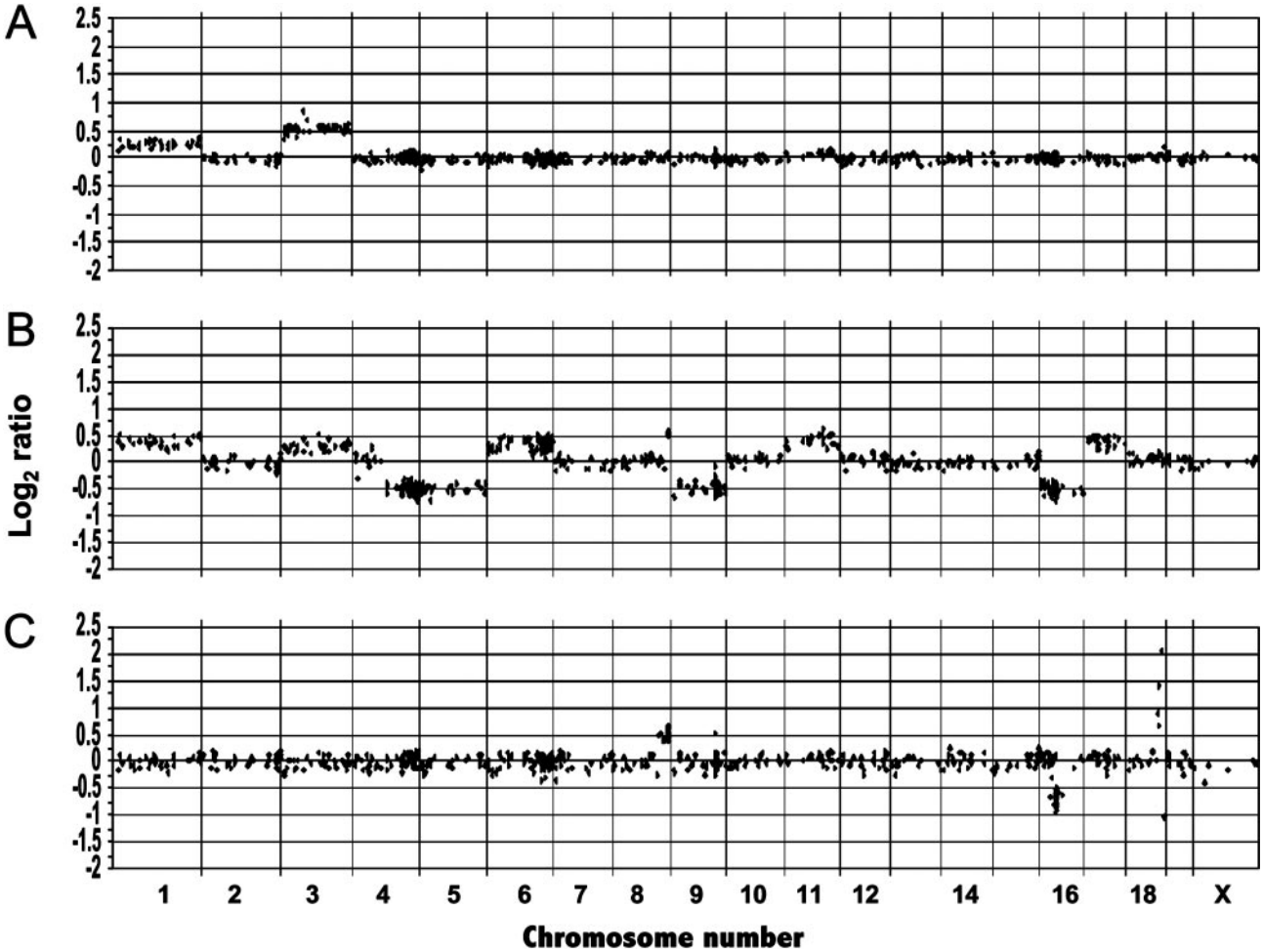

Fig. 1. Representative array CGH profiles for individual tumors. *A–C*, profiles for three tumors. Average $\log_2$ ratios were plotted for all clones based on chromosome position, with *vertical bars* representing the separation of chromosomes. *A*, one tumor with gains of chromosomes 3 and 1, a frequently observed pattern. *B*, deletion of distal chromosome 4; gain of chromosomes 1, 3, 6, 11, and 17; localized gain on chromosomes 8 and 18; and loss of chromosomes 5, 9, and 16. *C*, localized amplification of distal chromosome 18, localized gain on chromosome 8, and loss on chromosome 16.

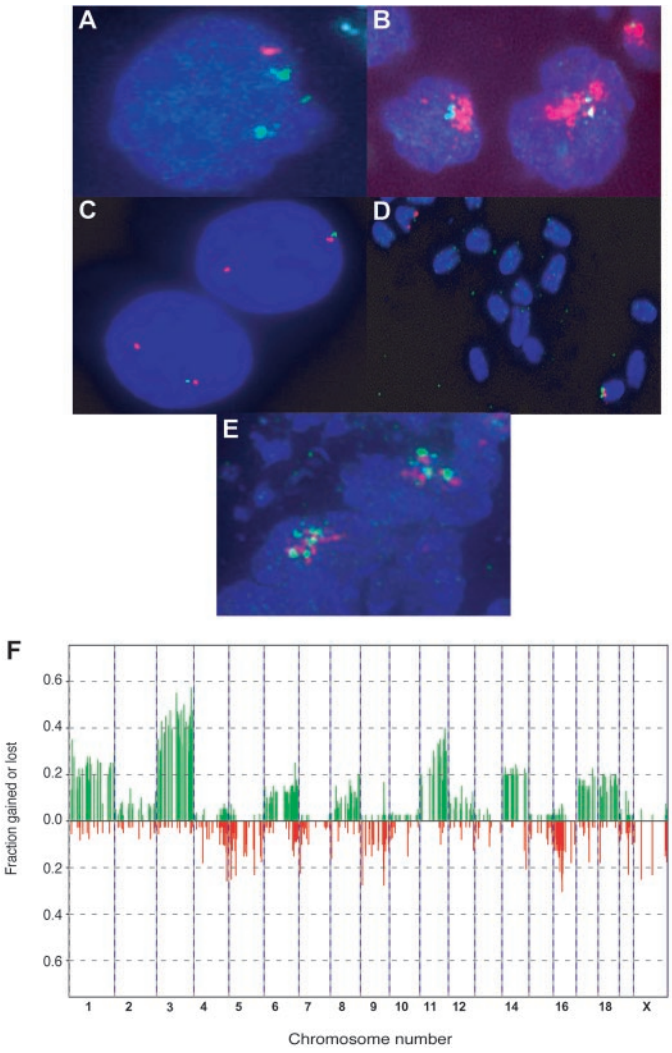

Fig. 2. FISH confirmation of localized abnormalities and overall frequencies of gain and loss observed by array CGH on 40 tumors. *A*, loss of a single copy of distal chromosome 4 in the tumor profiled in Fig. 1*B* (*red* is BAC RPCI-23-101G23, on distal chromosome 4; *green* is an unlinked control BAC RPCI-23-301L12). *B*, verification of amplified distal chromosome 18 in the tumor profiled in Fig. 1*C* (*red* is RPCI-23-16A3, the BAC at the peak of the amplicon; *green* is an unlinked control BAC RPCI-23-18M23). *C*, colocalization of transgenic MYCN probe with a probe on distal chromosome 18 in normal interphase fibroblasts from a mouse transgenic for *TH-MYCN* (*red* is RPCI-23-16A3; *green* is MYCN transgene). *D*, colocalization of probes from *C* in metaphase nuclei. *E*, coamplification of the MYCN transgene with distal chromosome 18 in the tumor profiled in Fig. 1*C*, using the same probes as in *C* and *D*. *E*, frequencies for all markers in all tumors. Clones are plotted based on physical mapping position (February 2002). Clones were scored as gained or lost according to "Materials and Methods." Positive frequency bars (*green*) represent gains (positive green:red ratio); negative bars (*red*) represent losses.

modifier analysis suggested to us that distal chromosome 18 was the site of *TH-MYCN* transgene integration.[8] Two-color FISH using a probe for the *TH-MYCN* transgene and the probe from Fig. 2*B* verified association of these two markers in interphase nuclei (Fig. 2*C*) and metaphase spreads (Fig. 2*D*) in fibroblasts from mice transgenic for *TH-MYCN*. To further define the linkage between the *MYCN* transgene and amplicon on chromosome 18, we performed two-color FISH against the tumor analyzed in Fig. 1*C*. This analysis revealed coamplification of *MYCN* and distal chromosome 18, as show in Fig. 2*E*.

A summary of array CGH analysis of 40 tumors is shown in Fig. 2*F*. Gains and losses for each arrayed clone were determined as described previously (20), revealing whole-chromosome gains of chromosomes 1 (25%), 3 (41%), 11 (29%), 14 (20%), 17 (15%), and 18 (17%). Whole chromosome losses were observed for chromosomes 5 (11%), 9 (10%), and 16 (14%). We also observed lower frequency gain of chromosomes 6 (12%), 8 (11%), 2 (6%), and 12 (7%), and losses of 15 (6%) and 19 (5%) were also observed (Table 1). Frequencies of chromosomal change were significantly nonhomogeneous (see "Materials and Methods"), suggesting differentially acting selective forces. Selected clones on chromosomes 1, 11, and 18 showed recurrent subchromosomal gain (Table 2).

AI Analysis Validates Observations by Array CGH. We had reported previously an AI screen using 46 markers across the 20 mouse chromosomes in tumors from this model (16). This analysis revealed imbalance on chromosomes 1, 3, 10, 11, 14, and 18 and showed an absolute association between imbalance of chromosomes 1 and 10 and a relative association between imbalance of chromosomes 1, 3, and 10. Most of the changes were imbalances of whole chromosomes.

In the current study, we further screened 96 markers for AI across chromosomes 1, 3, 10, 11, 14, and 18 (with control markers on chromosomes 2 and 13) on 32 tumors (see "Materials and Methods" for details). This study confirmed significant imbalance of markers on chromosomes 1 (highest frequency of imbalance 28%), 3 (38%), 11 (22%), 14 (31%), and 18 (41%). Average frequencies for all markers across each chromosome were: chromosome 1 (19%), 3 (29%), 11 (22%), 14 (32%), and 18 (40%; See supplementary data). The AI analysis revealed whole-chromosome copy number changes in most cases. All of these changes corresponded to chromosome gains according to array CGH (Fig. 1*D*). Consecutive, localized markers showing highest levels of AI on chromosomes 1 and 18 fell within 10 Mb of clones most frequently gained in the array CGH screen (data not shown).

Tumors Showing Partial Gain of Chromosome 11 Delineate a Minimal 15-Mb Region Orthologous to Human Chromosome 17q. Array CGH showed whole-chromosome gain of chromosome 11 in ~30% of tumors. Selected tumors gained only the distal half of this chromosome, which is orthologous to the region of human chromosome arm 17q implicated in 83% of human neuroblastoma (3). Fig. 3 illustrates the profile of chromosome 11 in three informative tumors. Horizontal dotted lines in each profile represent the cutoff of 3 SDs from the central distribution of all clones in each tumor, the threshold used to identify gain and loss of single clones. Vertical solid lines indicate the minimal gained region. This 15-Mb region of distal chromosome 11 corresponds to a segment of human chromosome 17q

Table 1 *Summary of whole-chromosome genetic changes*

Chromosome	Average AI[a]	Frequency of gain: array CGH[b]	Frequency of loss: array CGH[b]
1	19%	25.1%	2.4%
2	na	6.0%	2.1%
3	29%	41.0%	2.3%
4	na	1.0%	4.3%
5	na	1.3%	10.7%
6	na	11.7%	2.6%
7	na	0.8%	4.3%
8	na	11.4%	1.9%
9	na	1.4%	10.0%
10	na	2.3%	2.5%
11	12%	28.7%	1.5%
12	na	6.7%	2.1%
13	na	1.1%	2.9%
14	20%	19.8%	2.3%
15	na	2.9%	6.4%
16	na	0%	13.9%
17	na	15.1%	2.8%
18	28%	16.7%	1.5%
19	na	3.0%	5.4%
X	na	5.4%	17.5%

[a] Average frequency of imbalance of all markers across chromosome.
[b] Average frequency of gain/loss for all markers scored in ≥70% of tumors.

[8] C. S. H. and W. A. W., unpublished observations.

Table 2 *Localized regions of change on selected chromosomes*

Chromosome	Array CGH whole-chromosome gain frequency	Large locus (Mb position)	Minimal locus (Mb position)	Peak frequency	Human orthology	Genes
1 (gain)	25.1%	73–94	78–81	35%	2q: gained in 12% of NBL (3)	*Epha 4, Pax3, Dgat21, Kcne4, scg2, Serpine2*
3 (gain)	41.0%	60–130	86, 95, 119	45–55%	3q, 4q, 1p: Not gained in NBL	
11 (gain)	28.7%	101–122	107–113	40%	17q, 60–79 Mb: gained in 83% of NBL (3)	*Tlk 2, Mapt, Pecam, Rgs9, Gna13, Axin2, Prkca*
18 (gain)	16.7%	42–61, 70–81	53–61, 75–81	25%	5q: Not gained in NBL	*TH-MYCN* transgene
9 (loss)	10.0%	100–103	101.36–101.46	22.5%	3q: Not implicated in NBL	*Nck1, Stag1, Pccb*
16 (loss)	13.9%	32–40	36.7–37.0	27.5%	3q: Not implicated in NBL	*Gprc2a, Cd86, Slc5a2, Mc1s1*

from 62.2–80.7 Mb.[6] Human orthology was determined by homology of genes flanking the region in mouse, *Psmc5* on the proximal end (*PSMC5* in human), and *MCT4* on the distal end (*SLC16A3* in human). Importantly, regions immediately proximal to this position in mice correspond to a more proximal region of chromosome 17q, outside of the minimal region implicated in human disease (Fig. 3*D*).

Cluster Analysis of Array CGH Profiles. Using hierarchical clustering algorithms (28), we clustered the array CGH profiles from 40 tumors to reveal recurrent patterns of whole-chromosome copy number changes (Fig. 4*A*). We confirmed an interaction observed previously between gains of chromosomes 1 and 3 ($P \leq 0.006$). We also identified novel significant pair wise interactions between losses of chromosomes 5, 9, and 16 ($P \leq 0.001$ for each possible pair) and of chromosome 15 with all elements of this pair (with either 9 or 16, $P \leq 0.003$; with 5, $P \leq 0.02$). Gain of chromosome 11 also interacts with this set ($P \leq 0.026$, ≤ 0.051, and ≤ 0.137 for chromosomes 9, 5, and 16, respectively), as well as with gain of chromosome 1 ($P \leq 0.108$). *P*s were adjusted for multiple comparisons as described (29), and all comparisons with an adjusted $P < 0.5$ are shown in Table 3. Two-way interactions are represented graphically in Fig. 4*B*. To assess three chromosome interactions, we treated each significant pair wise interaction as a single event and compared the pair with other individual chromosomes. A highly significant complex emerged of all combinations of losses of chromosomes 5, 9, and 16 and gain of chromosome 11 ($P \leq 0.001$ for comparisons involving each chromosome) and 15 with all pairs in this group ($P \leq 0.007$). A separate complex, involving the gain of combinations of chromosomes 1, 3, and 6, showed less statistical significance after multiple test correction ($P \leq 0.1$; see Table 4 for all interactions with *P*s < 0.5). Interestingly, gain of chromosome 11 participates in both complexes. Attempts to cluster genetic profile with latency and location of tumor (abdominal, thoracic, and neck) demonstrated no significant association. Histological analysis of tumors revealed a narrow range of morphology and did not show significant variability to associate with genetic profiles.

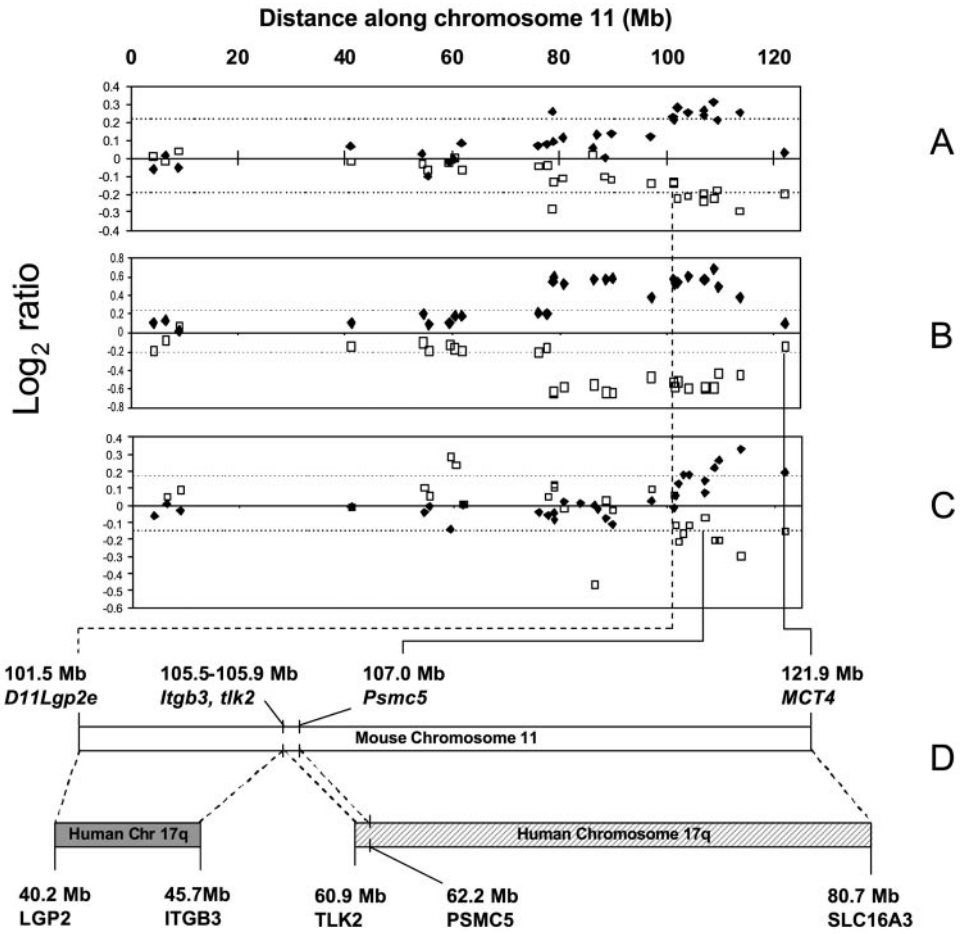

Fig. 3. Delineation of minimal region of gain on distal chromosome 11. *A–C,* individual profiles of three tumors with informative localized gains. *Dotted horizontal lines*, the stringent threshold used to identify gains. ♦, forward labeling hybridizations. □, reverse-fluor hybridizations. *D*, region of common gain among the three tumors is identified by *solid vertical lines* descending from flanking clones below the cutoff lines. Genes flanking the 15-Mb region in mouse (*Psmc5* and *MCT4*) were used to identify corresponding 18.5-Mb region on human chromosome 17q (human RefSeq gene *SLC16A3* is homologous to mouse *MCT4*). *Bars below*, orthology between mouse chromosome 11 and human 17. *Diagonal shaded box*, region gained in human neuroblastoma. *Vertical dashed line* (descending from flanking clones below the cutoff lines in *A*), a more extensive region of gain on mouse 11 defined by the tumor in *A*. This region corresponds to a more proximal section of human chromosome 17 (*solid gray box*) distinct from that implicated in human neuroblastoma.

DISCUSSION

Array CGH Analysis of Murine Neuroblastoma Confirms Regions of AI. Although neuroblastoma accounts for 15% of cancer-related deaths in childhood, relatively little is known about the genetic complexity of this disease. We therefore used the best characterized genetic mutation in this malignancy to model neuroblastoma in transgenic mice. Because targeted expression of *MYCN* to the peripheral neural crest leads to neuroblastoma, we hypothesize that mice transgenic for *TH-MYCN* provide a powerful tool to identify spontaneously arising mutations that contribute to the pathogenesis of these tumors. In addition, with the completed sequences of the human and mouse genomes (33–35), analysis of mouse tumors may narrow large regions of change in human tumors through analysis of orthology between the two genomes.

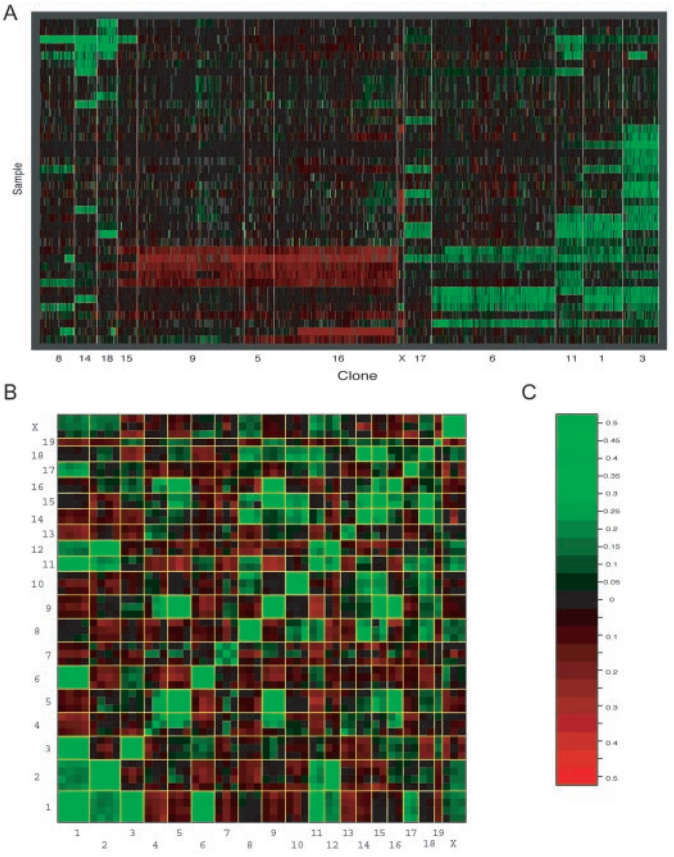

Fig. 4. Cluster and interaction analysis. *A*, two-way cluster display of normalized $\log_2$ ratio tumor profiles demonstrating concordant chromosomal changes. *Rows*, tumors; *columns*, BAC clones ordered by map position. Gain of material (positive $\log_2$ ratios) is represented in *green* and loss of material in *red* (the color scale of ratios from −0.5 to +0.5 is shown in 4*C*). Chromosomes were clustered based on rates of whole-chromosome change; samples were clustered based on individual $\log_2$ ratios of individual clones. *B*, display of average correlation of the clones binned by their genomic position. After data sets were normalized to median 0, cross-correlations were computed for all pairs of clones. To generate this figure, each chromosome was then subdivided into nonoverlapping 50-Mb bins, and the cross-correlations of the bins were calculated by averaging all of the cross-correlations for the clones falling into a given pair of bins. Degree of correlation ranges from negative (gain correlates with loss; *red*) to no correlation (*black*) to positive correlations (gain correlates with gain or loss with loss; *green*; the color scale from −0.5 to +0.5 is shown in 4*C*). *C*, color scale for *A* and *B*.

Table 3 *Two-way whole-chromosome interactions*

Chromosome 1	Chromosome 2	*P* (raw)	*P* (adj. minP)
5	9	0	0.001
5	16	0	0.001
9	16	0	0.001
9	15	2.00E-04	0.003
15	16	4.00E-04	0.005
5	15	8.00E-04	0.019
9	11	0.0013	0.026
5	11	0.0022	0.051
1	3	0.0055	0.101
1	11	0.0059	0.108
11	16	0.0071	0.137
1	6	0.0095	0.24
11	15	0.0149	0.295

Table 4 *Three-way whole-chromosome interactions*

Chromosome 1 (pair)	Chromosome 2 (pair)	Chromosome 3	*P* (raw)	*P* (adj. minP)
5	9	16	0	0.001
5	16	9	0	0.001
9	16	5	0	0.001
9	11	5	0	0.001
9	11	16	0	0.001
5	11	9	0	0.001
5	11	16	0	0.001
5	9	15	2.00E-04	0.007
9	16	15	2.00E-04	0.007
15	16	9	2.00E-04	0.007
5	15	9	2.00E-04	0.007
9	11	15	2.00E-04	0.007
5	16	15	4.00E-04	0.01
9	15	16	4.00E-04	0.01
5	15	16	4.00E-04	0.01
5	11	15	4.00E-04	0.01
9	15	5	8.00E-04	0.021
15	16	5	8.00E-04	0.021
5	9	11	0.0013	0.034
9	16	11	0.0013	0.034
1	3	6	0.0036	0.099
5	16	11	0.0071	0.19
9	15	11	0.0149	0.432
15	16	11	0.0149	0.432
5	15	11	0.0149	0.432

Our array CGH analysis confirmed all of the changes observed through AI screening of a subset of the same tumors, with the exception of a localized imbalance on chromosome 10 reported previously (16). Analysis of 14 markers along chromosome 10 showed no significant imbalance apart from the *D10MIT44* marker used in our original screen, which showed a unique localized imbalance in a significant number of tumors and an absolute association with imbalance of chromosome 1. This marker has been subsequently remapped to chromosome 1,[9] thereby explaining the obligatory association of imbalances on chromosomes 1 and 10 in this tumor set. One other marker on chromosome 10, *D10Mit136*, showed AI in 22% of samples, although markers <5 Mb on either side showed AI frequencies of <4%. Markers on chromosomes 1, 3, 11, 14, and 18 demonstrated significant imbalance, in agreement with the previous study and with trends observed in the array CGH analysis. In addition, the array CGH analysis confirmed previous observations using chromosome CGH of a different set of 21 tumors, showing similar trends of losses of mouse chromosomes 5, 9, 16, and X and gains of chromosomes 3, 11, and 17 (15).

Patterns of Localized Genetic Change in Murine Neuroblastoma Correlate with Changes Observed in Human Tumors and Other Mouse Models. Amplification of *MYCN* is specifically associated with loss of 1p36 and gain of 17q in human neuroblastoma and is inversely associated with loss of 11q (12–14, 36). Our study of the *TH-MYCN* model has allowed us to further refine the locus of genes on human chromosome 17q likely to contribute to the genesis of neuroblastoma. The mouse orthologue of human chromosome 17 is entirely contained on mouse chromosome 11,[10] which was gained in 30% of murine tumors. Furthermore, a 15-Mb region of chromosome 11 was gained with even higher frequency and corresponds to a region from 62.2 to 80.7 Mb on human chromosome 17q (Fig. 3). Human tumors show frequent

[9] Internet address: http://www.jax.org/resources/documents/cmdata.
[10] Internet address: http://www.ensembl.org/Mus_musculus/syntenyview.

translocation of 17q23.1-qter, which corresponds to 56–80 Mb on the human physical map (13). The human–mouse orthology thus narrows this region to the distal 18.5 Mb of chromosome 17q. Roughly 220 RefSeq genes map to this region in mice.[6] The 10-Mb peak of single clones showing the highest ratios in all three tumors includes ~37 RefSeq genes, including *Tlk 2*, a serine-threonine kinase involved in regulation of chromatin assembly (37). Importantly, *Tlk 2* has been identified as the closest gene distal to the breakpoint of a constitutional translocation in a patient with human neuroblastoma (38). This region also contains several cell adhesion genes, including *Pecam*, involved in angiogenesis (39); three G-proteins, *Rgs9*, *Gna13*, and *Axin2*, which interacts with the *Mapt* and *Wnt3* genes located proximally in the region (40, 41); and protein kinase C (*Prkca*). All of these genes are potential oncogenes in this region.

The mouse orthologue of human 1p36 includes the distal end of chromosome 4. We observed FISH-verified loss of a large portion of distal chromosome 4 in one tumor (Fig. 1*B*). In addition, one BAC, mapping to a region containing the human *p73* gene as verified by PCR, was lost in 13% of tumors, although this could not be verified by FISH (data not shown). Further investigation of this locus will help clarify its potential role in progression of *MYCN*-induced murine neuroblastoma.

Murine tumors showed simultaneous losses of chromosomes 5, 9, and 16 ($P \leq 0.001$). These three chromosomes share orthology with portions of human chromosome arms 3p, 4p, and 11q. Combined loss of human chromosomes 3p and 4p is common in stage 4 tumors, which also have 11q loss ($P = 1.10^{-6}$ and 0.016, respectively; Refs. 3 and 9), suggesting that a multichromosome interaction is conserved between species. Although loss of 11q reportedly occurs infrequently in human tumors with MYCN amplification, the smallest region of overlap in human tumors, from 11q14 to 11q23 (42), shares orthology with mouse chromosome 9. In addition, the smallest region of overlap from human chromosome 3pter-24[10] includes regions of mouse chromosomes 9 and 16. Gain of mouse chromosome 11, which parallels the most frequently observed genetic event in human neuroblastoma (7, 13), was significantly associated with loss of chromosomes 5, 9, and 16 ($P \leq 0.001$).

Losses of chromosomes 9 and 16 have also been observed in the *RIP-Tag*-induced mouse islet carcinoma model, suggesting a role for common tumor suppressors in distinct mouse models (20, 31). Peaks of frequent deletion in murine neuroblastoma localized to within 1 Mb of the most common regions of loss on chromosomes 9 and 16 in *RIP-Tag*-initiated tumors, regions that were represented by very high density of clones on the array. These regions, from 101 to 102 Mb on chromosome 9 and from 36 to 37 Mb on chromosome 16, both map to human chromosome 3q. The region on chromosome 9 includes the gene *Nck1*, which has been shown to interact with the *TrkB* gene (43). Expression of *TrkB* is associated with poor prognosis in human neuroblastoma (44). The region on chromosome 16 includes the mouse homologues of *EAF1*, an ELL-associated factor implicated in leukemia (45), and *HCLS1*, a gene down-regulated in ovarian cancers (46). More proximal regions of chromosome 16 map to chromosome 16p in humans, implicated in familial neuroblastoma (47).

Mouse chromosomes 1 and 3 share orthology with human chromosome arm 1q, which is frequently gained in advanced human neuroblastoma (48). Similarly, mouse chromosome 6, gained in 12% of tumors, has significant orthology with human chromosomes 7 and 12, gained in 50 and 15% of human cases, respectively (3). Human neuroblastomas also show gains of 18q in 30% of cases (3). This chromosome arm shares orthology with mouse chromosomes 1 and 18, both of which were gained in our study.

FISH validation of patterns seen by array CGH confirmed that the region of gain on chromosome 18 represents the site of integration of the *TH-MYCN* transgene (Fig. 2). The frequent gain of chromosome 18 in this model is consistent with data published previously demonstrating that doubling the gene dosage for the *MYCN* transgene leads to more aggressive malignancy (15, 49). We observed gains of chromosome 12, which contains the endogenous mouse *Nmyc* gene, in only 5% of samples. Amplification of endogenous *Nmyc* may not be necessary for tumorigenesis, however, given the presence of the overexpressed *MYCN* transgene.

Murine tumors initiated by the *TH-MYCN* transgene display a wide range of genetic aberrations with similarity to human neuroblastoma. Although the similarities between murine and human neuroblastoma suggest mutation in orthologous genes, specific validation to clarify the relevance of murine neuroblastoma to human disease awaits localization and identification of specific genes mutated in tumors from both species. Focus on chromosomes showing orthologous aberration in human tumors, particularly when paired with higher resolution human mouse genome orthology maps, should better characterize genes in candidate loci. Additional studies of subchromosomal gains and losses, and the interactions of loci on multiple chromosomes, should facilitate the identification of genetic pathways undiscovered previously in the progression of clinical disease.

ACKNOWLEDGMENTS

We thank Sujatmi Hariono and Nadya Milshteyn for technical assistance, Grace Kim for pathology review, and Nobumoto Tomioka for comments on this manuscript.

REFERENCES

1. Brodeur, G. M. Neuroblastoma: biological insights into a clinical enigma. Nat. Rev. Cancer, *3:* 203–216, 2003.
2. Brodeur, G. M., Seeger, R. C., Schwab, M., Varmus, H. E., and Bishop, J. M. Amplification of N-myc in untreated human neuroblastomas correlates with advanced disease stage. Science (Wash. DC), *224:* 1121–1124, 1984.
3. Vandesompele, J., Speleman, F., Van Roy, N., Laureys, G., Brinskchmidt, C., Christiansen, H., Lampert, F., Lastowska, M., Bown, N., Pearson, A., Nicholson, J. C., Ross, F., Combaret, V., Delattre, O., Feuerstein, B. G., and Plantaz, D. Multicentre analysis of patterns of DNA gains and losses in 204 neuroblastoma tumors: how many genetic subgroups are there? Med. Pediatr. Oncol., *36:* 5–10, 2001.
4. Vandesompele, J., Van Roy, N., Van Gele, M., Laureys, G., Ambros, P., Heimann, P., Devalck, C., Schuuring, E., Brock, P., Otten, J., Gyselinck, J., De Paepe, A., and Speleman, F. Genetic heterogeneity of neuroblastoma studied by comparative genomic hybridization. Genes Chromosomes Cancer, *23:* 141–152, 1998.
5. Lastowska, M., Nacheva, E., McGuckin, A., Curtis, A., Grace, C., Pearson, A., and Bown, N. Comparative genomic hybridization study of primary neuroblastoma tumors. United Kingdom Children's Cancer Study Group. Genes Chromosomes Cancer, *18:* 162–169, 1997.
6. Van Gele, M., Van Roy, N., Jauch, A., Laureys, G., Benoit, Y., Schelfhout, V., De Potter, C. R., Brock, P., Uyttebroeck, A., Sciot, R., Schuuring, E., Versteeg, R., and Speleman, F. Sensitive and reliable detection of genomic imbalances in human neuroblastomas using comparative genomic hybridisation analysis. Eur. J. Cancer, *33:* 1979–1982, 1997.
7. Plantaz, D., Mohapatra, G., Matthay, K. K., Pellarin, M., Seeger, R. C., and Feuerstein, B. G. Gain of chromosome 17 is the most frequent abnormality detected in neuroblastoma by comparative genomic hybridization. Am. J. Pathol., *150:* 81–89, 1997.
8. Vettenranta, K., Aalto, Y., Wikstrom, S., Knuutila, S., and Saarinen-Pihkala, U. Comparative genomic hybridization reveals changes in DNA-copy number in poor-risk neuroblastoma. Cancer Genet. Cytogenet., *125:* 125–130, 2001.
9. Breen, C. J., O'Meara, A., McDermott, M., Mullarkey, M., and Stallings, R. L. Coordinate deletion of chromosome 3p and 11q in neuroblastoma detected by comparative genomic hybridization. Cancer Genet. Cytogenet., *120:* 44–49, 2000.
10. Plantaz, D., Vandesompele, J., Van Roy, N., Lastowska, M., Bown, N., Combaret, V., Favrot, M. C., Delattre, O., Michon, J., Benard, J., Hartmann, O., Nicholson, J. C., Ross, F. M., Brinkschmidt, C., Laureys, G., Caron, H., Matthay, K. K., Feuerstein, B. G., and Speleman, F. Comparative genomic hybridization (CGH) analysis of stage 4 neuroblastoma reveals high frequency of 11q deletion in tumors lacking MYCN amplification. Int. J. Cancer, *91:* 680–686, 2001.
11. Cunsolo, C. L., Bicocchi, M. P., Petti, A. R., and Tonini, G. P. Numerical and structural aberrations in advanced neuroblastoma tumours by CGH analysis; survival correlates with chromosome 17 status. Br. J. Cancer, *83:* 1295–1300, 2000.
12. Maris, J. M., White, P. S., Beltinger, C. P., Sulman, E. P., Castleberry, R. P., Shuster, J. J., Look, A. T., and Brodeur, G. M. Significance of chromosome 1p loss of heterozygosity in neuroblastoma. Cancer Res., *55:* 4664–4669, 1995.
13. Meddeb, M., Danglot, G., Chudoba, I., Venuat, A. M., Benard, J., Avet-Loiseau, H., Vasseur, B., Le Paslier, D., Terrier-Lacombe, M. J., Hartmann, O., and Bernheim, A.

Additional copies of a 25 Mb chromosomal region originating from 17q23.1–17qter are present in 90% of high-grade neuroblastomas. Genes Chromosomes Cancer, *17:* 156–165, 1996.
14. Bown, N., Cotterill, S., Lastowska, M., O'Neill, S., Pearson, A. D., Plantaz, D., Meddeb, M., Danglot, G., Brinkschmidt, C., Christiansen, H., Laureys, G., Speleman, F., Nicholson, J., Bernheim, A., Betts, D. R., Vandesompele, J., and Van Roy, N. Gain of chromosome arm 17q and adverse outcome in patients with neuroblastoma. N. Engl. J. Med., *340:* 1954–1961, 1999.
15. Weiss, W. A., Aldape, K., and Bishop, J. M. Targeted expression of NMYC causes neuroblastoma in transgenic mice. Eur. Mol. Biol. Org. J., *16:* 2985–2995, 1997.
16. Weiss, W. A., Godfrey, T., Francisco, C., and Bishop, J. M. Genome-wide screen for allelic imbalance in a mouse model for neuroblastoma. Cancer Res., *60:* 2483–2487, 2000.
17. Solinas-Toldo, S., Lampel, S., Stilgenbauer, S., Nickolenko, J., Benner, A., Dohner, H., Cremer, T., and Lichter, P. Matrix-based comparative genomic hybridization: biochips to screen for genomic imbalances. Genes Chromosomes Cancer, *20:* 399–407, 1997.
18. Pinkel, D., Segraves, R., Sudar, D., Clark, S., Poole, I., Kowbel, D., Collins, C., Kuo, W. L., Chen, C., Zhai, Y., Dairkee, S. H., Ljung, B. M., Gray, J. W., and Albertson, D. G. High resolution analysis of DNA copy number variation using comparative genomic hybridization to microarrays. Nat. Genet., *20:* 207–211, 1998.
19. Snijders, A. M., Nowak, N., Segraves, R., Blackwood, S., Brown, N., Conroy, J., Hamilton, G., Hindle, A. K., Huey, B., Kimura, K., Law, S., Myambo, K., Palmer, J., Ylstra, B., Yue, J. P., Gray, J. W., Jain, A. N., Pinkel, D., and Albertson, D. G. Assembly of microarrays for genome-wide measurement of DNA copy number. Nat. Genet., *29:* 263–264, 2001.
20. Hodgson, G., Hager, J. H., Volik, S., Hariono, S., Wernick, M., Moore, D., Nowak, N., Albertson, D. G., Pinkel, D., Collins, C., Hanahan, D., and Gray, J. W. Genome scanning with array CGH delineates regional alterations in mouse islet carcinomas. Nat. Genet., *29:* 459–464, 2001.
21. Osoegawa, K., Tateno, M., Woon, P. Y., Frengen, E., Mammoser, A. G., Catanese, J. J., Hayashizaki, Y., and de Jong, P. J. Bacterial artificial chromosome libraries for mouse sequencing and functional analysis. Genome Res., *10:* 116–128, 2000.
22. Kent, W. J. BLAT–the BLAST-like alignment tool. Genome Res., *12:* 656–664, 2002.
23. Telenius, H., Pelmear, A. H., Tunnacliffe, A., Carter, N. P., Behmel, A., Ferguson-Smith, M. A., Nordenskjold, M., Pfragner, R., and Ponder, B. A. Cytogenetic analysis by chromosome painting using DOP-PCR amplified flow-sorted chromosomes. Genes Chromosomes Cancer, *4:* 257–263, 1992.
24. Jain, A. N., Tokuyasu, T. A., Snijders, A. M., Segraves, R., Albertson, D. G., and Pinkel, D. Fully automatic quantification of microarray image data. Genome Res., *12:* 325–332, 2002.
25. Yang, Y. H., Dudoit, S., Luu, P., Lin, D. M., Peng, V., Ngai, J., and Speed, T. P. Normalization for cDNA microarray data: a robust composite method addressing single and multiple slide systematic variation. Nucleic Acids Res., *30:* e15, 2002.
26. Snedeckor, G. W., and Cochran, W. G. (eds.). Statistical Methods, Ed. 8. Ames, IA, Iowa State University Press, 1989.
27. Ihaka, R., and Gentlemen, R. R. A language for data analysis and graphics. J. Comput. Graph. Stat., *5:* 299–314, 1996.
28. Hartigan, J. A. (ed.). Clustering Algorithms. New York: Wiley, 1975.
29. Westfall, P. H., and Young, S. S. Resampling-Based Multiple Testing: Examples and Methods for p-value Adjustment. New York: John Wiley & Sons, 1993.
30. MacGrogan, D., Levy, A., Bostwick, D., Wagner, M., Wells, D., and Bookstein, R. Loss of chromosome arm 8p loci in prostate cancer: mapping by quantitative allelic imbalance. Genes Chromosomes Cancer, *10:* 151–159, 1994.
31. Dietrich, W. F., Radany, E. H., Smith, J. S., Bishop, J. M., Hanahan, D., and Lander, E. S. Genome-wide search for loss of heterozygosity in transgenic mouse tumors reveals candidate tumor suppressor genes on chromosomes 9 and 16. Proc. Natl. Acad. Sci. USA, *91:* 9451–9455, 1994.
32. 2000 Report of the AVMA Panel on Euthanasia. J. Am. Vet. Med. Assoc., *218:* 669–696, 2001.
33. Consortium, I. H. S. Initial sequencing and analysis of the human genome. Nature (Lond.), *409:* 860–921, 2001.
34. Venter, J. C., Adams, M. D., Myers, E. W., Li, P. W., Mural, R. J., Sutton, G. G., Smith, H. O., Yandell, M., Evans, C. A., Holt, R. A., Gocayne, J. D., Amanatides, P., Ballew, R. M., Huson, D. H., Wortman, J. R., Zhang, Q., Kodira, C. D., Zheng, X. H., Chen, L., Skupski, M., Subramanian, G., Thomas, P. D., Zhang, J., Gabor Miklos, G. L., Nelson, C., Broder, S., Clark, A. G., Nadeau, J., McKusick, V. A., Zinder, N., Levine, A. J., Roberts, R. J., Simon, M., Slayman, C., Hunkapiller, M., Bolanos, R., Delcher, A., Dew, I., Fasulo, D., Flanigan, M., Florea, L., Halpern, A., Hannenhalli, S., Kravitz, S., Levy, S., Mobarry, C., Reinert, K., Remington, K., Abu-Threideh, J., Beasley, E., Biddick, K., Bonazzi, V., Brandon, R., Cargill, M., Chandramouliswaran, I., Charlab, R., Chaturvedi, K., Deng, Z., Di Francesco, V., Dunn, P., Eilbeck, K., Evangelista, C., Gabrielian, A. E., Gan, W., Ge, W., Gong, F., Gu, Z., Guan, P., Heiman, T. J., Higgins, M. E., Ji, R. R., Ke, Z., Ketchum, K. A., Lai, Z., Lei, Y., Li, Z., Li, J., Liang, Y., Lin, X., Lu, F., Merkulov, G. V., Milshina, N., Moore, H. M., Naik, A. K., Narayan, V. A., Neelam, B., Nusskern, D., Rusch, D. B., Salzberg, S., Shao, W., Shue, B., Sun, J., Wang, Z., Wang, A., Wang, X., Wang, J., Wei, M., Wides, R., Xiao, C., Yan, C., Yao, A., Ye, J., Zhan, M., Zhang, W., Zhang, H., Zhao, Q., Zheng, L., Zhong, F., Zhong, W., Zhu, S., Zhao, S., Gilbert, D., Baumhueter, S., Spier, G., Carter, C., Cravchik, A., Woodage, T., Ali, F., An, H., Awe, A., Baldwin, D., Baden, H., Barnstead, M., Barrow, I., Beeson, K., Busam, D., Carver, A., Center, A., Cheng, M. L., Curry, L., Danaher, S., Davenport, L., Desilets, R., Dietz, S., Dodson, K., Doup, L., Ferriera, S., Garg, N., Gluecksmann, A., Hart, B., Haynes, J., Haynes, C., Heiner, C., Hladun, S., Hostin, D., Houck, J., Howland, T., Ibegwam, C., Johnson, J., Kalush, F., Kline, L., Koduru, S., Love, A., Mann, F., May, D., McCawley, S., McIntosh, T., McMullen, I., Moy, M., Moy, L., Murphy, B., Nelson, K., Pfannkoch, C., Pratts, E., Puri, V., Qureshi, H., Reardon, M., Rodriguez, R., Rogers, Y. H., Romblad, D., Ruhfel, B., Scott, R., Sitter, C., Smallwood, M., Stewart, E., Strong, R., Suh, E., Thomas, R., Tint, N. N., Tse, S., Vech, C., Wang, G., Wetter, J., Williams, S., Williams, M., Windsor, S., Winn-Deen, E., Wolfe, K., Zaveri, J., Zaveri, K., Abril, J. F., Guigo, R., Campbell, M. J., Sjolander, K. V., Karlak, B., Kejariwal, A., Mi, H., Lazareva, B., Hatton, T., Narechania, A., Diemer, K., Muruganujan, A., Guo, N., Sato, S., Bafna, V., Istrail, S., Lippert, R., Schwartz, R., Walenz, B., Yooseph, S., Allen, D., Basu, A., Baxendale, J., Blick, L., Caminha, M., Carnes-Stine, J., Caulk, P., Chiang, Y. H., Coyne, M., Dahlke, C., Mays, A., Dombroski, M., Donnelly, M., Ely, D., Esparham, S., Fosler, C., Gire, H., Glanowski, S., Glasser, K., Glodek, A., Gorokhov, M., Graham, K., Gropman, B., Harris, M., Heil, J., Henderson, S., Hoover, J., Jennings, D., Jordan, C., Jordan, J., Kasha, J., Kagan, L., Kraft, C., Levitsky, A., Lewis, M., Liu, X., Lopez, J., Ma, D., Majoros, W., McDaniel, J., Murphy, S., Newman, M., Nguyen, T., Nguyen, N., Nodell, M., Pan, S., Peck, J., Peterson, M., Rowe, W., Sanders, R., Scott, J., Simpson, M., Smith, T., Sprague, A., Stockwell, T., Turner, R., Venter, E., Wang, M., Wen, M., Wu, D., Wu, M., Xia, A., Zandieh, A., and Zhu, X. The sequence of the human genome. Science (Wash. DC), *291:* 1304–1351, 2001.
35. Gregory, S. G., Sekhon, M., Schein, J., Zhao, S., Osoegawa, K., Scott, C. E., Evans, R. S., Burridge, P. W., Cox, T. V., Fox, C. A., Hutton, R. D., Mullenger, I. R., Phillips, K. J., Smith, J., Stalker, J., Threadgold, G. J., Birney, E., Wylie, K., Chinwalla, A., Wallis, J., Hillier, L., Carter, J., Gaige, T., Jaeger, S., Kremitzki, C., Layman, D., Maas, J., McGrane, R., Mead, K., Walker, R., Jones, S., Smith, M., Asano, J., Bosdet, I., Chan, S., Chittaranjan, S., Chiu, R., Fjell, C., Fuhrmann, D., Girn, N., Gray, C., Guin, R., Hsiao, L., Krzywinski, M., Kutsche, R., Lee, S. S., Mathewson, C., McLeavy, C., Messervier, S., Ness, S., Pandoh, P., Prabhu, A. L., Saeedi, P., Smailus, D., Spence, L., Stott, J., Taylor, S., Terpstra, W., Tsai, M., Vardy, J., Wye, N., Yang, G., Shatsman, S., Ayodeji, B., Geer, K., Tsegaye, G., Shvartsbeyn, A., Gebregeorgis, E., Krol, M., Russell, D., Overton, L., Malek, J. A., Holmes, M., Heaney, M., Shetty, J., Feldblyum, T., Nierman, W. C., Catanese, J. J., Hubbard, T., Waterston, R. H., Rogers, J., de Jong, P. J., Fraser, C. M., Marra, M., McPherson, J. D., and Bentley, D. R. A physical map of the mouse genome. Nature (Lond.), *418:* 743–750, 2002.
36. Seeger, R. C., Brodeur, G. M., Sather, H., Dalton, A., Siegel, S. E., Wong, K. Y., and Hammond, D. Association of multiple copies of the N-myc oncogene with rapid progression of neuroblastomas. N. Eng. J. Med., *313:* 1111–1116, 1985.
37. Sillje, H. H., and Nigg, E. A. Identification of human Asf1 chromatin assembly factors as substrates of Tousled-like kinases. Curr. Biol., *11:* 1068–1073, 2001.
38. Van Roy, N., Vandesompele, J., Berx, G., Staes, K., Van Gele, M., De Smet, E., De Paepe, A., Laureys, G., van der Drift, P., Versteeg, R., Van Roy, F., and Speleman, F. Localization of the 17q breakpoint of a constitutional 1;17 translocation in a patient with neuroblastoma within a 25-kb segment located between the ACCN1 and TLK2 genes and near the distal breakpoints of two microdeletions in neurofibromatosis type 1 patients. Genes Chromosomes Cancer, *35:* 113–120, 2002.
39. Ferrero, E., Belloni, D., Contini, P., Foglieni, C., Ferrero, M. E., Fabbri, M., Poggi, A., and Zocchi, M. R. Transendothelial migration leads to protection from starvation-induced apoptosis in CD34+CD14+ circulating precursors: evidence for PECAM-1 involvement through Akt/PKB activation. Blood, *101:* 186–193, 2003.
40. Stoothoff, W. H., Bailey, C. D., Mi, K., Lin, S. C., and Johnson, G. V. Axin negatively affects tau phosphorylation by glycogen synthase kinase 3beta. J. Neurochem., *83:* 904–913, 2002.
41. Katoh, M. WNT3-WNT14B and WNT3A-WNT14 gene clusters (Review). Int. J. Mol. Med., *9:* 579–584, 2002.
42. Maris, J. M., Guo, C., White, P. S., Hogarty, M. D., Thompson, P. M., Stram, D. O., Gerbing, R., Matthay, K. K., Seeger, R. C., and Brodeur, G. M. Allelic deletion at chromosome band 11q14–23 is common in neuroblastoma. Med. Pediatr. Oncol., *36:* 24–27, 2000.
43. Suzuki, S., Mizutani, M., Suzuki, K., Yamada, M., Kojima, M., Hatanaka, H., and Koizumi, S. Brain-derived neurotrophic factor promotes interaction of the Nck2 adaptor protein with the TrkB tyrosine kinase receptor. Biochem. Biophys. Res. Commun., *294:* 1087–1092, 2002.
44. Brodeur, G. M., Nakagawara, A., Yamashiro, D. J., Ikegaki, N., Liu, X. G., Azar, C. G., Lee, C. P., and Evans, A. E. Expression of TrkA, TrkB and TrkC in human neuroblastomas. J. Neuro-Oncol., *31:* 49–55, 1997.
45. Simone, F., Polak, P. E., Kaberlein, J. J., Luo, R. T., Levitan, D. A., and Thirman, M. J. EAF1, a novel ELL-associated factor that is delocalized by expression of the MLL-ELL fusion protein. Blood, *98:* 201–209, 2001.
46. Unoki, M., and Nakamura, Y. Growth-suppressive effects of BPOZ and EGR2, two genes involved in the PTEN signaling pathway. Oncogene, *20:* 4457–4465, 2001.
47. Maris, J. M., Weiss, M. J., Mosse, Y., Hii, G., Guo, C., White, P. S., Hogarty, M. D., Mirensky, T., Brodeur, G. M., Rebbeck, T. R., Urbanek, M., and Shusterman, S. Evidence for a hereditary neuroblastoma predisposition locus at chromosome 16p12–13. Cancer Res., *62:* 6651–6658, 2002.
48. Hirai, M., Yoshida, S., Kashiwagi, H., Kawamura, T., Ishikawa, T., Kaneko, M., Ohkawa, H., Nakagawara, A., Miwa, M., and Uchida, K. 1q23 gain is associated with progressive neuroblastoma resistant to aggressive treatment. Genes Chromosomes Cancer, *25:* 261–269, 1999.
49. Norris, M. D., Burkhart, C. A., Marshall, G. M., Weiss, W. A., and Haber, M. Expression of N-myc and MRP genes and their relationship to N-myc gene dosage and tumor formation in a murine neuroblastoma model. Med. Pediatr. Oncol., *35:* 585–589, 2000.